

See discussions, stats, and author profiles for this publication at: <https://www.researchgate.net/publication/23302012>

Enhanced Fluorescence Images for Labeled Cells on Silver Island Films

ARTICLE *in* LANGMUIR · NOVEMBER 2008

Impact Factor: 4.46 · DOI: 10.1021/la801749f · Source: PubMed

CITATIONS

35

READS

1,238

5 AUTHORS, INCLUDING:



Yi Fu

University of Maryland, Baltimore

53 PUBLICATIONS 1,711 CITATIONS

SEE PROFILE



Richard Y. Zhao

University of Maryland, Baltimore

136 PUBLICATIONS 1,775 CITATIONS

SEE PROFILE



Joseph R Lakowicz

University of Maryland Medical Center

877 PUBLICATIONS 42,252 CITATIONS

SEE PROFILE

Published in final edited form as:

Langmuir. 2008 November 4; 24(21): 12452–12457. doi:10.1021/la801749f.

Enhanced Fluorescence Images for Labeled Cells on Silver Island Films

Jian Zhang¹, Yi Fu¹, Dong Liang², Richard Y. Zhao^{2,4}, and Joseph R. Lakowicz¹

¹Center for Fluorescence Spectroscopy, University of Maryland School of Medicine, Department of Biochemistry and Molecular Biology, 725 West Lombard Street, Baltimore, MD 21201

²Division of Molecular Pathology, Department of Pathology, University of Maryland School of Medicine, 10 South Pine Street, Baltimore, MD 21201

³Department of Microbiology-Immunology, University of Maryland School of Medicine, 10 South Pine Street, Baltimore, MD 21201

⁴Institute of Human Virology, University of Maryland School of Medicine, 10 South Pine Street, Baltimore, MD 21201

Abstract

Silver island films (SIFs) were deposited on the glass substrates to serve as the supports. T-lymphocytic (*PM1*) cell lines were labeled by Alexa Fluor 680 dextran conjugates on the membranes or by YOYO in the nucleus, respectively. The fluorescence images of the cell lines were recorded in the emission intensity and lifetime using scanning confocal microscopy. The fluorescence signals by the fluorophores bound on the cell membranes were enhanced significantly by SIF supports as compared with on the glass. In addition to the increase in the intensity, there was a dramatic shortening of the emission lifetime. In contrast to the Alexa Fluor 680 fluorophores on the membranes, the YOYO fluorophores intercalated in the cell nucleus were not influenced significantly by the silver islands. This result can be interpreted by an effect of the distance on coupling between the fluorophores and metal particles: the fluorophores on the cell membranes are localized within but the fluorophores in the cell nucleus are beyond the region of metal-enhanced fluorescence. Thus, the metal supports can be used to improve the detection sensitivity to the target molecules on the cell surfaces when they are fluorescently labeled.

Keywords

silver island films (SIFs); Alexa Fluor 680; YOYO; dextran; T-lymphocytic (*PM1*) cell; scanning confocal microscopy; fluorescence image; emission intensity and lifetime

Fluorescence can be enhanced by one to three orders of magnitude when a fluorophore is localized near a nano-scale metal particle [1-5]. We describe this fluorescence enhancement on the metal surface as metal-enhanced fluorescence (MEF). The occurrence of MEF is primarily due to a near-field interaction of a fluorophore with an EM field around a metal particle that is induced by the incident light [6-8]. In this report we use the metal particles deposited on the solid supports, which are called the metal island films [9], as the support to detect the fluorescence images of the labeled cell lines. The metal island films, especially the silver island films (SIFs), have been shown to couple with the fluorophores and enhance the emission intensity when the fluorophores are localized within an optimal distance from the

surfaces of SIFs [10]. Because of their favorable effects, SIFs have been extensively used in fluorescence assays or single molecule detection for the biological functionalities, e.g. DNAs and proteins [11,12].

In recent years, the molecular fluorescent imaging to the cell lines has been developed rapidly due to a wide application of confocal microscopy and the availability of a large number of probes, including organic fluorophores, quantum dots, fluorescent nanoparticles, etc [13,14]. This imaging technology has shown a great promise for elucidating signaling pathways and performing disease diagnosis at the single molecular level when they are bound with the targets on the cell surfaces [15,16]. In most cases, the organic dyes are used as the fluorescent imaging agents. However, these organic fluorophores often display the emission signals of low intensity relative to the background from the autofluorescence of cell lines [17]. Moreover, the emission lifetimes of most organic fluorophores are ranged in 2 - 4 ns, close to the lifetimes of backgrounds from the cell autofluorescence [18]. Thus, it is difficult to separate the emission signals by the labeled targets from the whole cell images. In addition, the organic fluorophores are known to display the emission signals with poor photostability and strong photoblinking [19], so it is also of importance to develop novel technology to improve the photostability and reduce the photoblinking of the fluorophore to satisfy the requirements in the cell imaging.

We suggest using the metal plasmon-coupled probes (PCPs) instead of the regular organic fluorophores as the molecular agents in the cell imaging [20,21]. In this study, the metal nanoparticles especially the silver nanoparticles were synthesized and the organic fluorophores were bound on these metal particles. The bound fluorophores were separated from the surfaces of metal cores with the organic linkers or peptides to avoid the quenching from the metal cores to the bound fluorophores. These fluorescent metal particles were found to display the emission signals hundreds folds brighter than the single organic fluorophores, which are mostly due to the fluorophore-metal coupling interaction. The lifetime of bound fluorophores were shortened dramatically on the metal particles. By the brighter emission signals and shorter lifetime, these metal probes were observed more clearly on either the cell fluorescence intensity or lifetime images when bound on the cell surfaces. In addition, the fluorescence images of cell lines labeled by these PCPs were shown to have better photostability as compared with those by the regular organic fluorophores. By using the lifetime images of PCPs, we even can separate the single emission spots that appear to correspond to single target molecules [21]. This observation is very difficult when the regular organic fluorophores are used in the measurements. Thus, the metal-enhanced fluorescence can be regarded as a new strategy in developing a more sensitive detection technology in the cell imaging technology.

A recent report from Moal, et al, described to monitor the cell image on the metal mirror surfaces and the fluorescence signals from the organic dyes on the cell surfaces are increased by 4 folds by the metal substrate [22]. In the present report, we develop an efficient approach to image the labeled cell lines based on the previously discovered and reported phenomena. Instead of the silver mirror, we use the silver islands in this case as the support that is known to display a more efficient enhancement to the emission signals from the nearby fluorophores. In addition, beside the emission intensities, the lifetimes of bound fluorophores on the cells are also monitored to outline the cell images in the lifetime factor. Third, beside the cell surfaces, we also label the cell nucleus to study the effect of distance between the fluorophore and metal nanoparticle on the metal-enhanced fluorescence. Finally, we present clearly the influence from the metal substrate to the photostability of the bound fluorophores on the cell surfaces as well as in the nucleus. The organic fluorophore of Alexa Fluor 680 was used to label the cell surfaces and YOYO to label the cell nucleus in this case. SIFs have been demonstrated to excite the fluorophores in a wide wavelength from UV to near IR region [9], so the used fluorophores are expected to be coupled efficiently with the metal substrate. The cell images were monitored in the emission intensity and lifetime using the scanning confocal

microscopy, and the images on SIFs were compared with those collected on the glass slides to investigate the influences from the metal substrates to the fluorophores localized on the cell membranes or in the cell nucleus.

Experimental section

All reagents and spectroscopic grade solvents were used as received from Sigma-Aldrich. Alexa Fluor 680 dextran conjugate (MW 3,000, 0.6-0.7 dye / molecule) are commercially available from Invitrogen. T-lymphocytic (*PM1*) cell was obtained through the AIDS Research and Reference Reagent Program, the National Institute of Health. Nanopure water ($>18.0 \text{ M } \Omega\text{cm}^{-1}$) purified using Millipore Milli-Q gradient system, was used in all experiments. Oligonucleotides (TCCACACACCACTGGCCATCTTG and AGGTGTGTGGTGACCGGTAGAAC) were synthesized by the Biopolymer Laboratory in University of Maryland School of Medicine.

Preparing silver island film (SIF)

Silver island films (SIFs) were deposited on the cleaned glass coverslips by reduction of silver nitrate as reported previously [23]. The formed silver island films are greenish and nonreflective. Only one side of each slide was coated with SIFs. The SIFs were dipped in 1.0 mM N-(2-mercaptopropionyl) glycine (abbreviated as tiopronin) water solution for 30 min to coat SIFs with a monolayer of thiolate amino acid. These silver particles are typically 100-500 nm across and 70 nm high covering about 20% of the surfaces of coverslips.

Cell culture

The T-lymphocytic *PM1* cell line, which is a colonial derivative of HUT 78, was separated by ficoll-hypaque density gradient centrifugation. They were grown in the RPMI-1640 culture medium (Sigma) supplemented with 10% (v/v) heat-inactivated fetal bovine serum (Atlanta Biologicals Inc. GA) and contained 200 units/ml penicillin, 200 units/ml streptomycin (Invitrogen) and recombinant human interleukin (100U/ml) (Roche, Indianapolis, Indiana, USA) for 6 days prior to fluorescent labeling. The number of cells was counted to be *ca.* 5×10^6 cells / ml.

Labeling cell surfaces and nucleus

PM1 cell membranes were fluorescently labeled suspending in 500 μL aliquots of 1 pM Alexa 680-Dextran conjugates in 10 mM PBS buffer solutions at pH 7.2 for 1 h [24,25]. *PM1* cell nucleus were fluorescently labeled suspending in 500 μL aliquots of 1 pM YOYO in 10 mM PBS buffer solutions at pH 7.2 for 1 h [26]. All labeled cell samples were washed three times with PBS buffer solution, respectively, before casting on the glass coverslips for fluorescence image measurements.

Preparing measurement samples

All measurement samples were immobilized on glass coverslips with or without the coated silver islands. 10 nM oligonucleotides (TCCACACACCACTGGCCATCTTG and AGGTGTGTGGTGACCGGTACAAC) were hybridized in 10 mM PBS buffer solution [26]. 50 nM YOYO dyes were then added into buffer solution to intercalate into the hybridized duplexes to saturation. We cast a buffer solution with 10 nM Alexa Fluor 680 dextran conjugates or YOYO intercalated DNA molecules on the surfaces of coverslips with or without silver islands coating for the free dyes measurements. For the cell samples, we cast 20 μL suspensions of labeled cell lines on the surfaces of coverslips with or without silver islands coating. These samples were dried in air them at room temperature.

Spectra measurements

All image measurements were performed using a time-resolved confocal microscope (MicroTime 200, PicoQuant) [27]. A single mode pulsed laser diode (635 nm for Alexa Fluoro 680 or 470 nm for YOYO) was used as the excitation light. The collimated laser beam was spectrally filtered by an excitation filter (D637/10 for Alexa Fluoro 680 or D467/10 for YOYO, Chroma) before directing into an inverted microscope (Olympus, IX 71). An oil immersion objective (Olympus, 100 \times , 1.3NA) was used to focus laser light and collect fluorescence signal. The fluorescence that passed a dichroic mirror (Q655LP, Chroma) was focused onto a 75 μ m pinhole for spatial filtering to reject out-of-focus signals and then reached the single photon avalanche diode (SPAD) (SPCM-AQR-14, Perkin Elmer Inc). Images were recorded by raster scanning (in a bidirectional fashion) the sample of the incident laser with a pixel integration of 0.6 ms. The excitation power into the microscope was maintained at less than 1 μ W. The data was stored in a time-tagged-time-resolved (TTR) mode, which allows recording every detected photon with its individual timing information. Instrument Response Function (IRF) widths of about 300 ps FWHM were obtained in combination with a pulsed diode laser, which permits the recording of sub-nanosecond fluorescence lifetimes extendable to less than 100 ps with deconvolution. Lifetimes were estimated by fitting to a χ^2 value of less than 1.2 and with a residuals trace that was fully symmetrical about the zero axis. All measurements were performed in a dark compartment at room temperature.

Results and Discussion

SIFs were freshly prepared in this case and protected with the terminal-carboxylic acid thiolate ligands, so they should exist as the silver instead of the oxide when the cell fluorescence images were monitored by the confocal microscopy. It was confirmed by the wavelengths of their plasmon resonance at near 450 nm on the extinction spectra. It was observed that the formed silver island films in this method were greenish and none-reflective, and according our previous report the silver particles as the islands in this case were typically 100-500 nm across and 70 nm high [10]. Thus, we expect the fluorophores of Alexa Fluor 680 and YOYO used in this study can be enhanced efficiently by the silver substrate.

Figure 1 shows the images of Alexa Fluor 680 dextran conjugates on the glass and SIF upon excitation using a laser source at 635 nm. Because each dextran molecule contains average less than one dye, most detection images of dextran sample displayed a typical single molecule behavior with one-step photobleaching on either glass or SIFs. One emission spot corresponds to one single dextran molecule. It was shown that the emission spots on SIFs were 8-fold brighter than those on the glass, indicating that these fluorophores were coupled with the metal substrate to induce an efficient metal-enhanced fluorescence [10]. Simultaneously, the lifetime of fluorophores was found to significantly shorten from 1.8 ns on glass to 0.8 ns on SIFs further implying the coupling interaction of the fluorophores with the metal substrate.

Alexa Fluor 680 dextran conjugates were expected to adhere on the cell surfaces by molecule fusion [24]. The labeled cell samples were cast on the SIFs and the fluorescence images were recorded using scanning confocal microscopy in both intensity and lifetime as compared with those on the glass (upper panel in Figure 2). It was shown that the intensities of fluorophores are much brighter on the silver films (Figure 2). We selected some areas of the images with relatively high brightness on the glass to estimate the intensity ratio of these areas over the overall cell backgrounds, and the values were ranged in 2 - 3. Contrarily, the emission spots became much brighter on the metal support and the intensity ratio of the emission spots over the overall cell background was found to increase to as high as 10 folds for the same labeled cell sample. This effect is probably due to the coupling effect of the membrane-bound probes with the metal supports.

Besides the fluorescence intensity images, we also recorded the lifetime images of the labeled cells (down panel in Figure 2). It is known that the metal-enhanced fluorescence is a complicated process, where the metal particle affects the both excitation of the fluorophore as well as the intrinsic decay rate of fluorophore emission. The emission enhancement is reflected through an increase of the intrinsic decay rate for the fluorophore near the metal surface, which is represented by a change of the fluorophore lifetime [10]. It is interesting to notice that the overall fluorescence backgrounds by the cell autofluorescence are influenced insignificantly by SIFs but the emission spots by the adhered fluorophores on the cell surfaces were obviously shortened relative to those on the glass (lower panel in Figure 2). The intensity decays of these emission spots from the labeled cells on SIFs were analyzed using a dual exponential model and the lifetime components were obtained to be 3.0 and 1.0 ns, respectively. The longer component can be considered to contribute from the autofluorescence of cell lines and the shorter component from the fluorophores on the cell surfaces. The mean average lifetime of these emission spots is estimated to be 2.0 ns, smaller than that on the glass (2.5 ns). The lifetime change with the substrate can also be reflected by the lifetime histogram over the whole images (Figure 3), on which a lifetime maximum is observed for each cell sample. Comparing the cell sample cast on the glass, the lifetime maximum of the sample on SIFs is shortened from 2.7 ns to 2.2 ns. Thus, we conclude that the metal support can provide more information on the cell images when the emission spots from the targets on the cell surfaces become more countable.

A shorter lifetime can be advantageous because of a less time for photochemistry of fluorophore while in the excited state, and thus more excitation-emission cycles prior to photobleaching [27]. Thus, in this case, the fluorophores adhered on the cell surfaces are expected to display better photostability on the metal support as compared with those on the glass [28]. This prediction was verified in the experiment using the time trace monitoring to the emission spots on the cell images (Figure 4). It was shown that the emission intensity of a typical spot displays a continuous decay with irradiation time until complete elimination within 10 seconds on the glass, but the emission intensity is reduced to 1/3 only under the same irradiation conditions on SIFs indicating that the photostability for the fluorophores adhered on the cell surfaces is lengthened at least 3-fold by the metal support. Based on above results, we can conclude that the fluorophores adhered on the cell surfaces can be interacted efficiently by the silver particles on the slides.

Beside the fluorophores on the cell surfaces, we are also interested in the metal-enhancement effect to the interior labeled cells. The experiments were carried out by intercalating YOYO into DNA molecules in the cell nucleus, and then cast the labeled cell samples on the silver substrate to compare with those on the glass. The YOYO dyes in the nuclei labeled cells were excited by a laser source at 470 nm. We first confirm the fluorescence enhancement effect of metal islands to YOYO dyes. The YOYO were intercalated into the DNA duplexes to saturation and cast on the silver islands and glass substrates, respectively. It was shown that the images of YOYO intercalated DNA molecules were larger than those of Alexa Fluor 680 dextran conjugates (Figure 5), which was due to the multiple intercalations of dyes in one DNA duplex. It is known that one intercalated YOYO molecule may occupy 4-5 bps of DNA duplex chain. In this case, the DNA duplex has 23 bps so it contains about 5 YOYO molecules. The time trace profile for the labeled DNA duplex showed a gradual intensity decay on either the glass or SIFs confirming the existence of multiple fluorophores on one DNA duplex (Figure 4). For the fluorescence intensity, it was shown that the emission spots by the intercalated YOYO were 7-fold brighter on the silver islands than those on the glass indicating that occurrence of metal enhancement indeed. For the fluorescence lifetime, similar to the Alexa Fluor 680 dextran conjugates, the YOYO-DNA complexes also displayed a significant shortening of lifetime from 2.8 ns on the glass to 1.1 ns on the silver islands.

We labeled the nucleus of *PMI* cells with YOYO, which were expected to intercalate into the DNA duplexes in the cell nucleus [26]. The nuclei labeled cell sample was cast on the glass and SIF, respectively. It is shown that the nuclei labeled cell lines can be imaged well by confocal microscopy on both the glass and SIFs supports. However, in contrast to the membrane labeled cell sample, the nuclei labeled cell sample on the metal supports displayed only insignificant difference on both the intensity and lifetime images from those on the glass (Figure 6). This result is confirmed by the lifetime histogram for nuclei labeled cell images (Figure 7), on which the lifetime maximum 2.4 ns on the silver islands is well consistent with the value on the glass. We also monitor the time-trace profile to the emission spots on the nuclei labeled cell images (Figure 8), indicating that the fluorescence signals are not influenced by the metal support indeed.

The silver island films can be used to enhance the emission of the fluorophores with a wide emission wavelength. In this case, we confirm that the fluorescence by either Alex Fluor 680 or YOYO can be enhanced by SIFs. However, after labeling on the cell lines, these two fluorophores were found to display definitely spectral differences on the metal support. The reason is due to the different labeling positions of them on the cell lines. The Alexa Fluor 680 dextrans were most likely adhered on the cell membranes but the YOYO dyes were bound in the nucleus of cells. Thus, we can conclude that the factor of distance from the fluorophore to the silver islands instead of the fluorophore itself takes the effect to the difference for the fluorophore on the cell surfaces or in the nucleus.

It is known that the fluorescence is enhanced due to at least two effects; an increase in the electric field near the metal particle caused by incident light and an increase in radiative decay rate of the fluorophore by the metal particle. The first factor provides a stronger excitation rate and the second factor changes the quantum yield and lifetime of fluorophore. We thus can write an apparent fluorescence enhancement factor (G_{app}) as product of two factors: excitation (G_{ex}) and quantum yield (G_{QY}) [8],

$$G_{app} \sim G_{ex} G_{QY} \quad (1)$$

An increase in the rate of emission is not expected to change the decay time of a fluorophore. In the contrast, an increase in the radiative decay rate of a fluorophore will decrease the lifetime because of an increase in the rate of radiative decay. Hence, the intensity decay provides information on the fluorescence enhancement. For a free-space emission of an excited fluorophore, the quantum yield (Q_0) and lifetime (τ_0) can be expressed as,

$$Q_0 = \Gamma / (\Gamma + k_{nr}) \quad (2)$$

$$\tau_0 = (\Gamma + k_{nr})^{-1} \quad (3)$$

where Γ is a radiative decay rate and k_{nr} is non-radiative decay rate of fluorophore. For a fluorophore near a metal particle, both the radiative and non-radiative decay rates are altered and given by $\Gamma + \Gamma_m$ for the radiative rate and $k_{nr} + k_m$ for the non-radiative rate, in which Γ_m and k_m are the additional radiative and non-radiative rate due to the metal substrate. The quantum yield Q_m and lifetime τ_m of the fluorophore near the metal substrate thus become [10]

$$Q_m = \frac{\Gamma + \Gamma_m}{\Gamma + \Gamma_m + k_{nr} + k_m} = \frac{\Gamma(1+\gamma)}{\Gamma(1+\gamma) + k_{nr} + k_m} \quad (4)$$

$$\tau_m = \frac{1}{\Gamma + \Gamma_m + k_{nr} + k_m} = \frac{1}{\Gamma(1+\gamma) + k_{nr} + k_m} \quad (5)$$

These equations show that an increase in the radiative decay rate will increase the quantum yield and decrease the lifetime of a fluorophore.

However, it is known that the fluorescence is enhanced only when the fluorophore is localized at an optimal distance close to the surface of metal nanoparticle that is in a range of 5 to 30 nm [12,23]. Otherwise, the fluorescence enhancement becomes negligible. This fact has been confirmed by either theoretical simulations or experimental results from us [12,27] and other research groups [7]. For the current case, because the membrane of the cell line is about 7 nm thick, some fluorophores on the cell membranes that are adhered to the metal substrate may be localized within the enhancement region. Thus, the emission signals from the surface fluorophores become stronger in this study. However, the YOYO dyes are completely bound in the cell nucleus that is expected to localize beyond the region of metal-enhanced fluorescence. Thus, the fluorescence signals cannot be enhanced significantly by the metal substrate.

We are also concerned on the cytotoxicity of metal supports to the cells lines in culture [28]. Although the silver particles can be used as the broad-spectrum antimicrobial agents, in fact, the cytotoxicity of these silver particles is due to their surface properties [29]. When the surfaces of silver particles are nearly free, they can interact strongly with cells and kill them. However, in this case, we have coated the silver island surfaces with a monolayer of thiolate amino acid, which displays a good chemical stability in buffer solution. Thus, only a low cytotoxicity is expected on the silver island film for the cell culture. In order to demonstrate this point, we cultured HEK 293 cell lines on the silver islands, showing an even higher counting number of cell on the silver islands than on the glass, indicating the silver islands indeed display a low cytotoxicity as the support. Because of a strong emission signal, a short lifetime, and a better photostability in the cell imaging, as well as a low cytotoxicity in the cell culture, we expect the silver island films can be used to improve the detection sensitivity for the target molecules on the cell membranes.

Acknowledgements

This research was supported by grants from NIH (HG-00255, EB006521, and EB00682 to JRL) and research support from the University of Maryland Medical Center (RZ).

References

1. Sokolov K, Chumanov G, Cotton TM. *Anal. Chem* 1998;70:3898–3905. [PubMed: 9751028]
2. Shen Y, Swiatkiewicz J, Lin T-C, Markowicz P, Prasad PN. *J. Phys. Chem. B* 2002;106:4040–4042.
3. Yu F, Persson B, Lofas S, Knoll W. *J. Am. Chem. Soc* 2004;126:8902–8903. [PubMed: 15264814]
4. Bruzzone S, Malvaldi M, Arrighini GP, Guidotti C. *J. Phys. Chem. B* 2005;109:3807–3812. [PubMed: 16851429]
5. Stoermer RL, Keating CD. *J. Am. Chem. Soc* 2006;128:13243–13254. [PubMed: 17017805]
6. Kelly KL, Coronado E, Zhao LL, Schatz GC. *J. Phys. Chem. B* 2003;107:668–677.
7. Mertens H, Koenderink AF, Polman A. *Phys. Rev. B* 2007;76(115123):1–12.

8. Lakowicz, JR. Principles of Fluorescence Spectroscopy. Vol. 3rd edition. Kluwer Academic/Plenum Publishers; New York: 2006.
9. Ghosh SK, Pal T. Chem. Rev 2007;107:4797–4862. [PubMed: 17999554]
10. Lakowicz JR. Anal. Biochem 2005;337:171–194. [PubMed: 15691498]
11. Sabanayagam CR, Lakowicz JR. Nucleic Acids Res 2007;35:e13. [PubMed: 17169999]
12. Zhang J, Malicka J, Gryczynski I, Leonenko Z, Lakowicz JR. J. Phys. Chem. B 2005;109:7969–7975. [PubMed: 16851931]
13. Dunn RC. Chem. Rev 1999;99:2891–2928. [PubMed: 11749505]
14. Ambrose WP, Goodwin PM, Jett JH, Van Orden A, Werner JH, Keller RA. Chem. Rev 1999;99:2929–2956. [PubMed: 11749506]
15. Weissleder R, Tung CH, Mahmood U, Bogdanov A. Nature Biotechnol 1999;17:375–378. [PubMed: 10207887]
16. Chen I, Ting AY. Current Opinion in Biotech 2005;16:35–40.
17. Nagano T, Yoshimura T. Chem. Rev 2002;102:1235–1270. [PubMed: 11942795]
18. Knemeyer J-P, Hertzen D-P, Sauer M. Anal. Chem 2003;75:2147–2153. [PubMed: 12720354]
19. Rosenthal SJ, Tomlinson I, Adkins EM, Schroeter S, Adams S, Swafford L, McBride J, Wang Y, DeFelice LJ, Blakely RD. J. Am. Chem. Soc 2002;124:4586–4594. [PubMed: 11971705]
20. Zhang J, Fu Y, Lakowicz JR. Bioconjugate Chem 2007;18:800–805.
21. Zhang J, Fu Y, Liang D, Nowaczyk K, Zhao RY, Lakowicz JR. Nano Lett 2008;8:1179–1186. [PubMed: 18341300]
22. Moal, E. Le; Fort, E.; Lévêque-Fort, S.; Cordelières, FP.; Fontaine-Aupart, M-P.; Ricolleau, C. Biophys. J 2007;92:2150–2161. [PubMed: 17172306]
23. Lakowicz JR, Shen Y, Gryczynski Z, D'Auria S, Gryczynski I. Biochem. Biophys. Res. Commun 2001;286:875–879. [PubMed: 11527380]
24. Blumenthal R, Clague MJ, Durell SR, Epand RM. Chem. Rev 2003;103:53–70. [PubMed: 12517181]
25. Germershaus O, Merdan T, Bakowsky U, Behe M, Kissel T. Bioconjugate Chem 2006;17:1190–1199.
26. Zhang J, Fu Y, Lakowicz JR. Langmuir 2007;23:11734–11739. [PubMed: 17914851]
27. Zhang J, Fu Y, Chowdhury MH, Lakowicz JR. J. Phys. Chem. C 2008;112:18–26.
28. Fu Y, Zhang J, Lakowicz JR. Langmuir 2008;24:3429–3433. [PubMed: 18278953]
29. Elechiguerra JL, Burt JL, Morones JR, Camacho-Bragado A, Gao X, Lara HH, Yacaman MJ. J. Nanobiotech 2005;3:1477–1486.

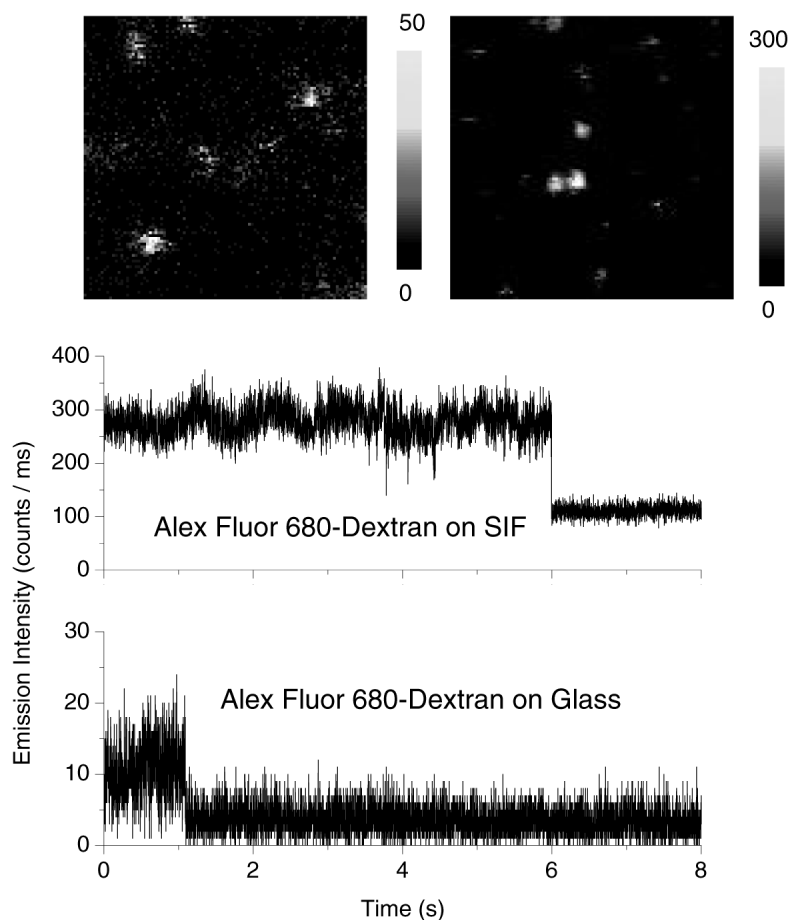


Figure 1.

Upper panel: representative emission intensity images of Alexa Fluor 680 dextran conjugates on the glass coverslips and on SIF, respectively. Lower panel: the time trace profiles of Alexa Fluor 680 dextran conjugates on the glass coverslips and on SIF, respectively. The images were acquired by a scanning confocal microscopy. The scales of diagrams are $5 \times 5 \mu\text{m}$. The resolution is 200×200 pixels with an integration of 0.6 ms/pixel.

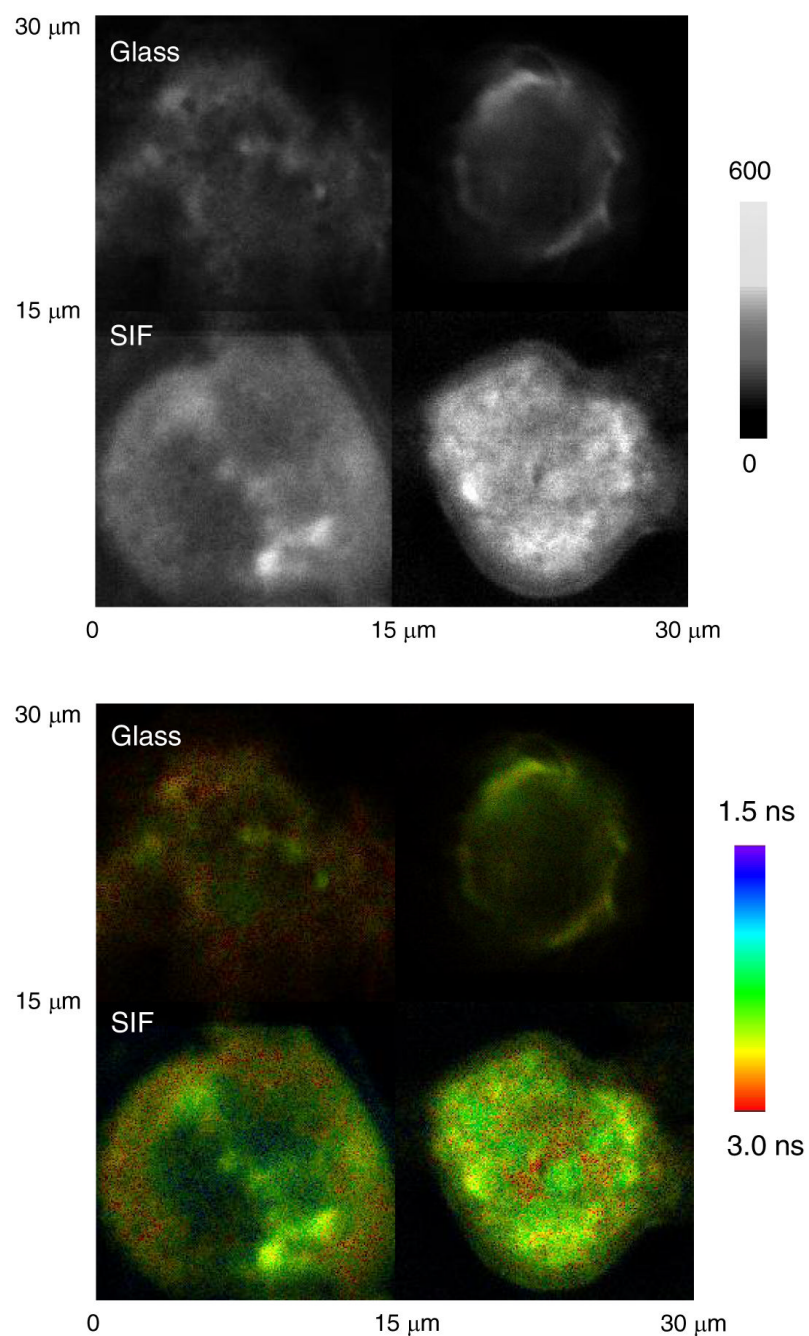


Figure 2.

Upper panel: representative emission intensity images of *PM1* cells labeled by Alexa Fluor 680 dextran conjugates adhered on the cell membranes on the glass coverslips and on SIF, respectively. Lower panel: corresponding lifetime images of intensity images on upper panel. The scales of diagrams are $15 \times 15 \mu\text{m}$. The resolution is 400×400 pixels with an integration of 0.6 ms/pixel.

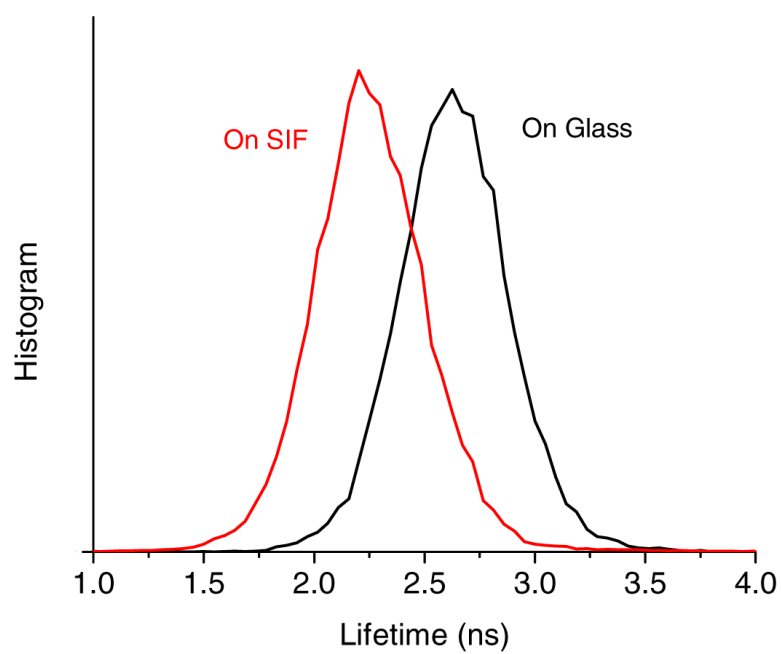


Figure 3. Histograms of lifetime on the membrane labeled *PMI* cells by Alexa Fluor 680 dextran conjugates on the glass coverslips and on SIF, respectively.

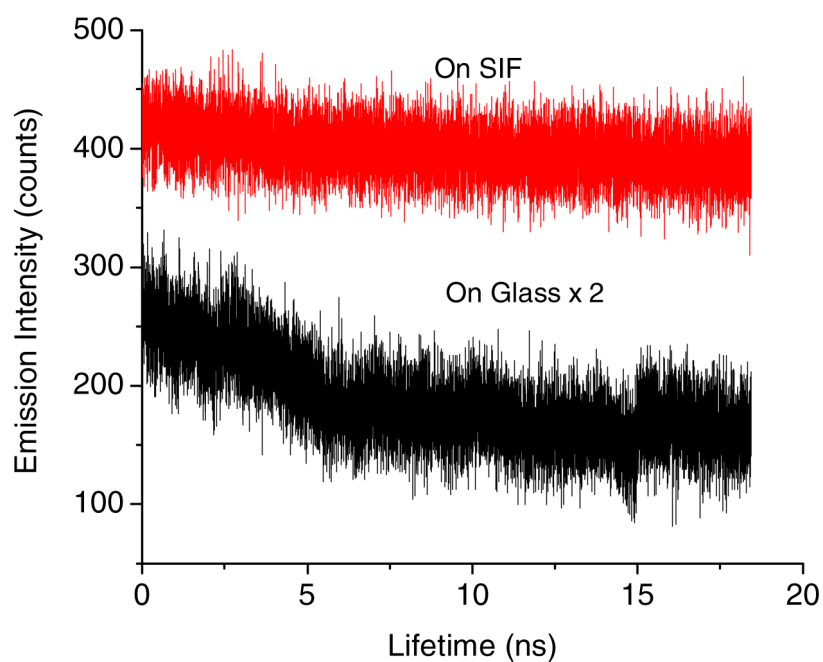


Figure 4. Respective time trace profiles for the emission spots of adhered Alexa Fluor 680 on the cell surfaces on the glass coverslips and on SIF, respectively.

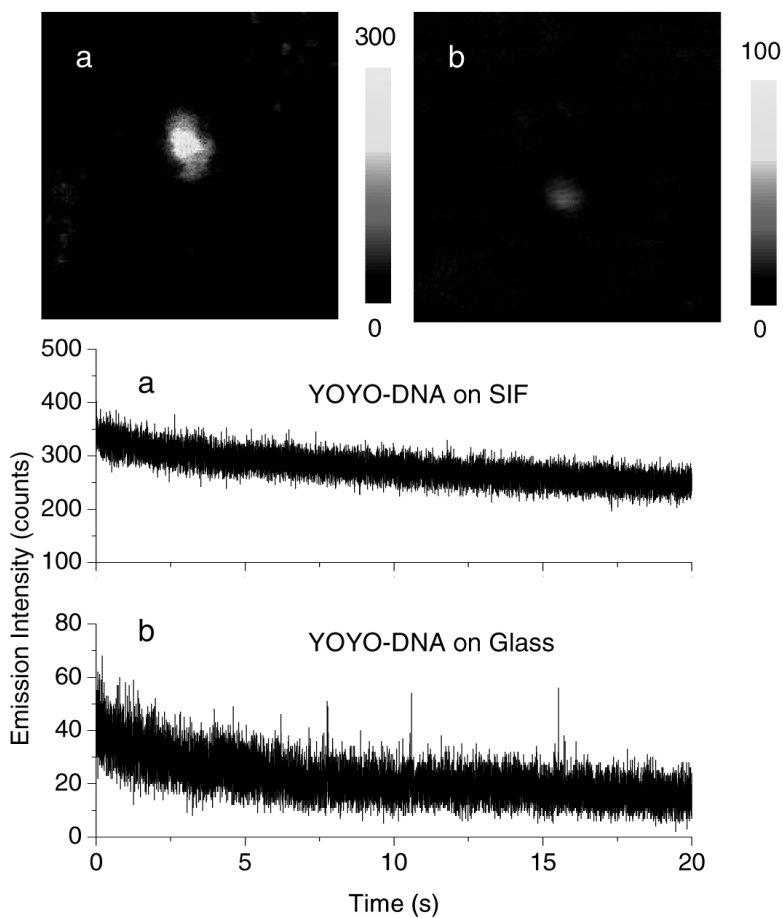


Figure 5.

Upper panel: representative emission intensity images of YOYO bound DNA duplexes on the glass coverslips and on SIF, respectively. Lower panel: the time trace files of YOYO intercalated DNA duplexes on the glass coverslips and on SIF, respectively. The images were acquired by a scanning confocal microscopy. The scales of diagrams are $5 \times 5 \mu\text{m}$. The resolution is 200×200 pixels with an integration of 0.6 ms/pixel.

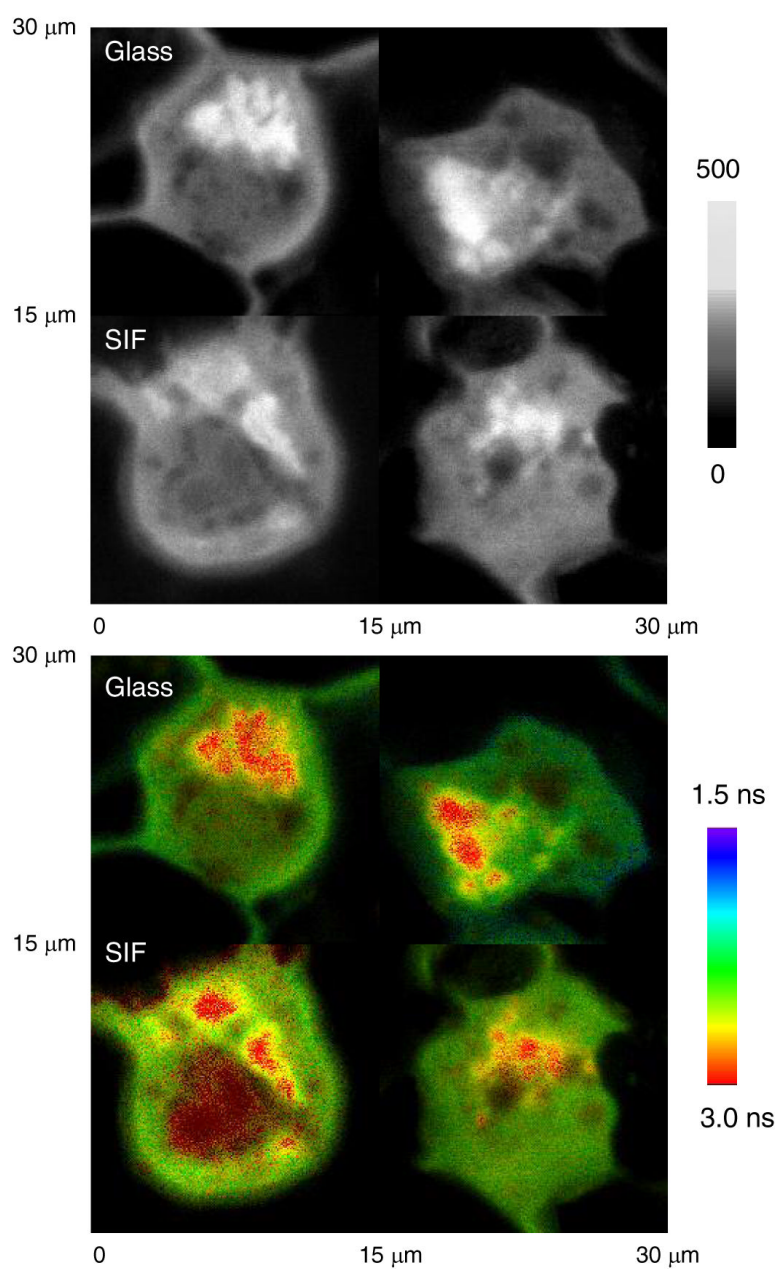


Figure 6.

Upper panel: representative emission intensity images of *PM1* cells labeled by YOYO bound in cell nucleus on the glass coverslips and on SIF, respectively. Lower panel: corresponding lifetime images of intensity images on upper panel. The scales of diagrams are $15 \times 15 \mu\text{m}$. The resolution is 400×400 pixels with an integration of 0.6 ms/pixel.

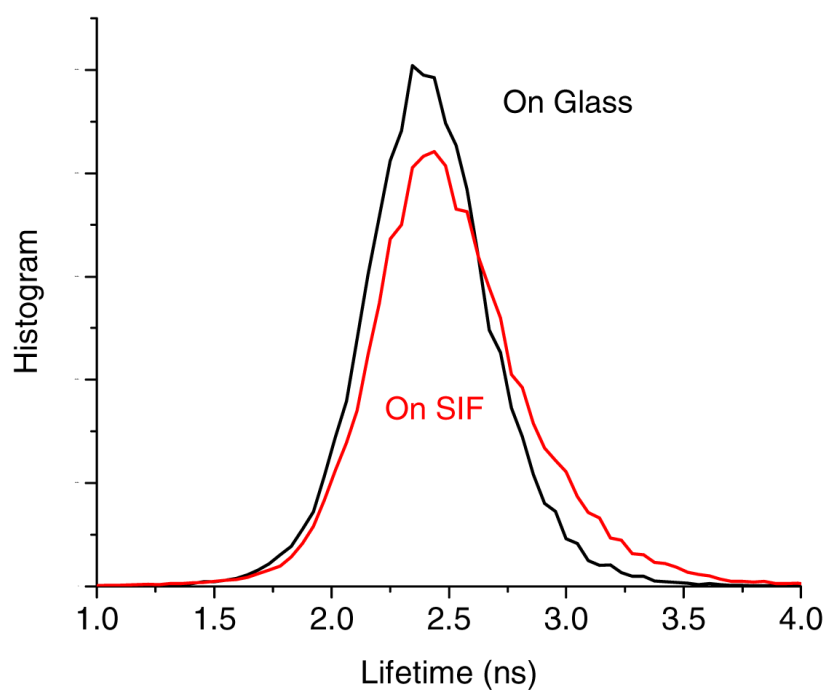


Figure 7. Histograms of lifetime on the nuclei-labeled cells line by YOYO on the glass coverslips and on SIF, respectively.

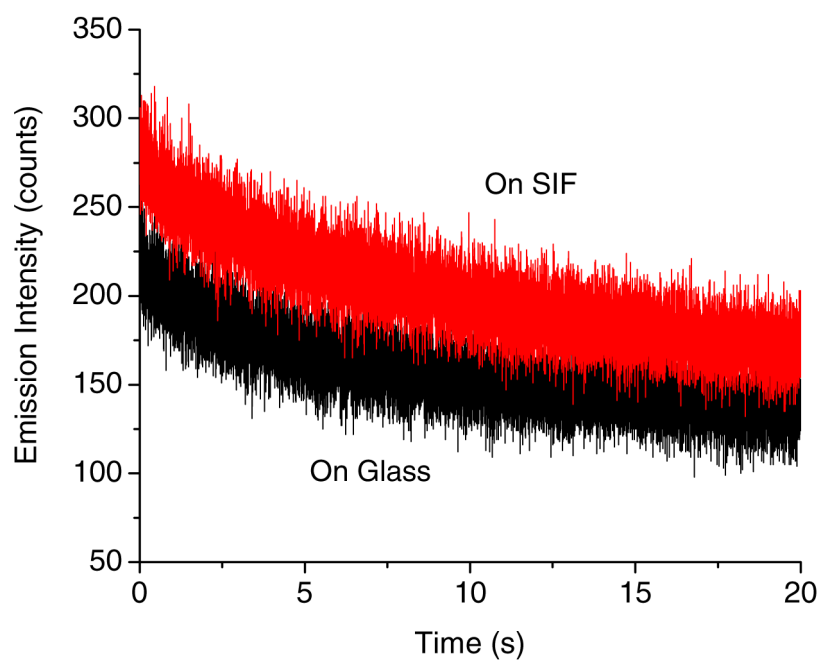


Figure 8. Respective time trace profiles for the emission spots of intercalated YOYO on the cell nucleus on the glass coverslips and on SIF, respectively.